Received: 28 March 2022 | Revised: 8 September 2022 | Accepted: 14 November 2022 | Published on: 13 December 2022

DOI: 10.1111/tra.12874

RESEARCH ARTICLE

Traffic WILEY

AP2S1 regulates APP degradation through late endosome–lysosome fusion in cells and APP/PS1 mice

Qi-Xin Wen[1] | Biao Luo[1] | Xiao-Yong Xie[1] | Gui-Feng Zhou[1] | Jian Chen[1] | Li Song[1] | Yue Liu[1] | Shi-Qi Xie[1] | Long Chen[1] | Kun-Yi Li[1] | Xiao-Jiao Xiang[2] | Guo-Jun Chen[1,3]

[1]Department of Neurology, The First Affiliated Hospital of Chongqing Medical University, Chongqing Key Laboratory of Major Neurological and Mental Disorders, Chongqing Key Laboratory of Neurology, Chongqing, China

[2]Department of Nuclear Medicine, The Second Affiliated Hospital of Chongqing Medical University, Chongqing, China

[3]Institute for Brain Science and Disease, Chongqing Medical University, Chongqing, China

Correspondence
Xiao-Jiao Xiang, Department of Nuclear Medicine, The Second Affiliated Hospital of Chongqing Medical University, 74 Linjiang Road, Chongqing 400010, China.
Email: 17723297891@163.com

Guo-Jun Chen, Department of Neurology, The First Affiliated Hospital of Chongqing Medical University, Chongqing Key Laboratory of Major Neurological and Mental Disorders, Chongqing Key Laboratory of Neurology, 1 Youyi Road, Chongqing 400016, China.
Email: woodchen2015@163.com

Funding information
Chongqing Education Commission, Grant/Award Number: KJZD-K201900404; National Nature Science Foundation of China, Grant/Award Number: 81971030; Postgraduate Research and Innovation Project of Chongqing, Grant/Award Number: CYB19146; National Nature Science Foundation of China, Grant/Award Number: 82201578

Abstract

AP2S1 is the sigma 2 subunit of adaptor protein 2 (AP2) that is essential for endocytosis. In this study, we investigated the potential role of AP2S1 in intracellular processing of amyloid precursor protein (APP), which contributes to the pathogenesis of Alzheimer disease (AD) by generating the toxic β-amyloid peptide (Aβ). We found that knockdown or overexpression of AP2S1 decreased or increased the protein levels of APP and Aβ in cells stably expressing human full-length APP695, respectively. This effect was unrelated to endocytosis but involved lysosomal degradation. Morphological studies revealed that silencing of AP2S1 promoted the translocalization of APP from RAB9-positive late endosomes (LE) to LAMP1-positive lysosomes, which was paralleled by the enhanced LE-lysosome fusion. In support, silencing of vacuolar protein sorting-associated protein 41 (VPS41) that is implicated in LE-lyso fusion prevented AP2S1-mediated regulation of APP degradation and translocalization. In APP/PS1 mice, an animal model of AD, AAV-mediated delivery of AP2S1 shRNA in the hippocampus significantly reduced the protein levels of APP and Aβ, with the concomitant APP translocalization, LE-lyso fusion and the improved cognitive functions. Taken together, these data uncover a LE-lyso fusion mechanism in APP degradation and suggest a novel role for AP2S1 in the pathophysiology of AD.

KEYWORDS
Adapter protein 2, Sigma subunit, Alzheimer disease, APP, Aβ, Endosome–lysosome fusion

1 | INTRODUCTION

Amyloid precursor protein (APP) is the only source of β-amyloid peptide (Aβ), which forms the characteristic amyloid plaques in Alzheimer disease (AD).[1] The proteolytic cleavage of APP involves the enzymatic activity of β-site APP cleaving enzyme 1 (BACE1) and γ-secretase, leading to the generation of the N-terminal soluble APPβ (sAPPβ), β-COOH-terminal fragment (CTFβ) and Aβ.[2] Genetic mutations of APP cause early-onset familial AD,[3] and abnormalities in APP processing might trigger the loss of neuronal connectivity early in AD.[4]

The enzymatic processing of APP and amyloidogenesis are paralleled by intracellular trafficking.[5] APP at cell surface is rapidly internalized into early endosome (EE), where it is trafficked to late endosome (LE) and lysosome for degradation.[6] Evidences have suggested that several genetic risk factors for AD are functionally related to endo-lysosomal regulation.[7,8] For instance, deficiency of CD2-associated protein (CD2AP) impairs lysosomal degradation of APP and favors Aβ generation.[9] Sortilin-related receptor with A-type repeats (SORL1) directly binds to APP and promotes the retrograde transport from endosome to trans-Golgi network (TGN), thus reducing APP processing and Aβ production in endosome.[10,11] It is hypothesized that the disrupted endo-lysosomal function is tightly coupled with APP in the development of AD.[12,13]

Adaptor protein 2 (AP2) is a heterotetrameric complex assembled by large α (AP2A1/AP2A2) and β2 (AP2B1) adaptins, one medium μ2 (AP2M1) subunit and one small σ2 (AP2S1) subunit.[14] It is well-established that AP2 subunits cooperatively control the initiation and stabilization of clathrin-coated pits, thus regulating clathrin-mediated endocytosis.[15] However, evidences have shown that among the four subunits of AP2, AP2M1 inhibits amyloidogenesis by regulating BACE1 trafficking[16] in addition to APP endocytosis.[17] AP2A1 could promote autophagic clearance of CTFβ through protein–protein interaction,[18] suggesting that the functions of different AP2 subunits are not completely identical. Thus, it might be important to explore how AP2S1 is involved in APP processing.

In this study, we found that knockdown of AP2S1 resulted in the decreased protein levels of APP and Aβ, which was different from the reported function of AP2M1 and AP2A1. We further defined that the function of AP2S1 was closely associated with LE-lyso fusion and lysosomal degradation mechanisms, in both cultured cells and APP/PS1 mice. Thus, our results uncovered a previously unappreciated role for AP2S1 in APP trafficking and amyloidogenesis.

2 | MATERIALS AND METHODS

2.1 | Antibodies and reagents

Antibodies for Western blotting were as follow: AP2S1 (ab128950, Abcam, 1:1000), APP-full length and CTFs (A8717, Sigma, 1:1000), BACE1 (ab2077, Abcam, 1:1000), sAPP-β (SIG-39138, Biolegend, 1:500), VPS41 (ab181078, Abcam, 1:1000), VPS16 (17776-1-AP, Proteintech, 1:1000), GAPDH (Proteintech, 1:10000). Horseradish peroxidase-conjugated anti-mouse (AB_2722565, 1:5000) and anti-rabbit (AB_2722564, 1:5000) secondary antibodies were purchased from Proteintech (Wuhan, China). Antibodies for immunofluorescence included: APP (MAB348, Sigma, 1:200), Aβ (MOAB-2, Novus Biologicals, 1:1000), EEA1 (#2411, 1:200), GM130 (#12480, 1:200), RAB9 (#5118, 1:200), LAMP1 (#9091, 1:100) were purchased from Cell Signaling Technology. Alexa Fluor 488-labeled Goat Anti-Rabbit (A0428, 1:200), Cy3-l-abeled Goat Anti-Rabbit (A0516, 1:200) and Alexa Fluor 647-labeled Goat Anti-Mouse (A0473, 1:200) secondary antibodies were purchased from Beyotime (Shanghai, China). Pitstop2 (HY-115604), dynasore (HY-13863), chloroquine (CQ, HY-17589A), bafilomycin A1 (BafA1, HY-100558), β-secretase inhibitor LY2811376 (HY-10472), α-secretase inhibitor GI254023X (HY-19956) and γ-secretase inhibitor DAPT (HY-13027) were purchased from MCE (Monmouth Junction, NJ, USA).

2.2 | Cell culture and transfection

HEK-APP and SH-SY5Y-APP cells (stably expressing full-length human amyloid-beta precursor protein 695) were created as described previously.[19,20] Cells were cultured in the DMEM (Gibco, Cat#11965092) or DMEM/F12 (Gibco, Cat#11220033) medium, supplemented with 10% fetal bovine serum (Hyclone, Cat#SV3008703) and 200 mg/mL of G418 (Sigma-Aldrich, Cat#N6386). All cells were incubated in a humidified incubator at 37°C with 5% CO2. Human AP2S1 plasmid and control vector were purchased from Youbio (Changsha, China). The siRNA oligonucleotides for human AP2S1, VPS16 and VPS41 were purchased from GenePharma (Shanghai, China). Non-targeting siRNA was adopted as the negative control. The following human siRNA oligonucleotide sequences were used: siAP2S1-1: CCGGAACUUUAAGAUCAUU; siAP2S1-2: GACCUGGU GUUCAACUUCU; siAP2S1-3: UCGUGGAGGUCUUAAACGA. These sequences were all effective in reducing AP2S1 and APP protein levels (Figure S1) and siAP2S1-2 sequence was selected for further siAP2S1 or shAP2S1 experiments in human cells. Other human siRNA sequences included siVPS16: GCCAGGGCACAAGCCCAGAAGAAGU; and siVPS41: UGACAUAGCAGCACGCAAAUU. HEK-APP cells were transfected with Lipofectamine™ 2000 (Invitrogen, Cat#11668019), and SH-SY5Y-APP cells were transfected with Lipofectamine RNAiMAX Transfection Reagent (Invitrogen, Cat#13778075) or Lipofectamine™ 3000 Transfection Reagent (Invitrogen, Cat#L3000015) in OptiMEM Reduced Serum Media (Gibco, Cat#31985088) according to the manufacturer's protocol.

2.3 | Western blotting

Animal tissues and cellular samples were digested in ice-cold RIPA buffer (Beyotime, Cat#P0013B) containing 0.5% sodium deoxycholate, 1% Triton X-100, 0.1% SDS, 1 mM EDTA, 150 mM NaCl and 50 mM Tris, supplemented with protease inhibitors (Dingguo, Cat#WB-0181) and

phosphatase inhibitors (Beyotime, Cat#P1081), followed by centrifugation at 13000 rpm for 20 min at 4°C. The soluble and insoluble proteins and sAPPβ were extracted as described previously.[19,21] BCA Protein Assay Kit (Beyotime, Cat#P0011) was used to measure protein concentrations. Samples were separated on 8% SDS-PAGE or 16.5% Tris-tricine gels, and were transferred to 0.22 μm polyvinylidene fluoride (PVDF) membranes (Bio-Rad, Cat#162-0177). Protein blots were visualized with chemiluminescence detection reagent kit (Affinity, Cat#KF8003) and captured by Fusion FX5 image analysis system (Vilber Lourmat, France). Relative protein intensities were calculated using Quantity One software (Bio-Rad, CA).

2.4 | Immunofluorescence

Brain sections or cultured cells on coverslips were washed with ice-cold PBS and fixed with 4% paraformaldehyde for 30 min at 37°C, then permeabilized with 0.3% Triton X-100 for 10 min at room temperature, blocked with 10% normal goat serum for 1 h at 37°C and incubated with the primary antibody in 5% BSA at 4°C overnight. Samples were washed with PBS three times and incubated with the appropriate fluorescent secondary antibody for 1 h, then mounted with DAPI Fluoromount-G (Southern Biotech, USA). Images were captured using a laser scanning confocal microscope (Leica TCS SP8 X, Germany). Quantification of immunofluorescence intensity and colocalization was performed using Image-Pro Plus 6.0 software (Media Cybernetics, USA).

2.5 | Enzyme-linked immunosorbent assay (ELISA) for Aβ40 and Aβ42

Soluble and insoluble Aβ40 and Aβ42 in animals were collected as described previously.[19] The levels of human Aβ40 and Aβ42 were measured by the ELISA kits following manufacturer's instructions (Elabscience, Wuhan, China).

2.6 | Dextran uptake assay

SH-SY5Y-APP cells were pretreated with dynasore or Pitstop2 or vehicle control (DMSO 1:2000) for indicated time, respectively. FITC-dextran (0.5 mg/mL, Sigma) was then applied to cell medium for 45 min at 37°C. After washing with PBS, cells were fixed with 4% paraformaldehyde and stained with DAPI.[22] Fluorescent images were captured by fluorescent microscope (Nikon, Japan), and FITC-dextran intensity was quantified by Image J software.

2.7 | Construction and imaging of APP-mKeima

MKeima is a coral-derived acid-stable fluorescent protein emitting different colored signals at acidic and neutral pH,[23] which can be used as a reporter of cargo delivery to lysosomes.[16] To generate APP-mKeima plasmid, mKeima-Red plasmid (Addgene, #54597) was linearized by PCR (primers: 5′-GTGAGTGTGATCGCTAAACAAATGA-3′ and 5′-CATGGTGGCGACCGGTGG-3′), and human APP695 sequence was PCR amplified from pcDNA3.1-APP695 (synthesized by the Yiobio) (primers: 5′-ATCCACCGGTCGCCACCATGCTGCCCGGTTTGGCACTG-3′ and 5′-TGTTTAGCGATCACACTCACCTAGTTCTGCATCTGCTCAAAGAACT-3′). Then the APP695 fragment was cloned into mKeima-Red plasmid by ClonExpress Ultra One Step Cloning Kit (Vazyme Biotech, Cat# C115-01). Plasmid sequence was verified by DNA sequencing.

SH-SY5Y cells were transfected with APP-mKeima and shAP2S1 plasmids for 48 h, and then imaged under confocal microscopy that was equipped with a 63× oil DIC objective. MKeima fluorescence was obtained using two excitation filters (550 and 438 nm), and the fluorescence intensity at 438 nm and 550 nm of excitation were measured using the Image J software after the background subtraction.

2.8 | Transmission electron microscopy (TEM)

The TEM samples were prepared as previously reported.[24] In brief, the samples were fixed in 0.1 M cacodylate buffer including 4% paraformaldehyde and 2% glutaraldehyde for 2 h at room temperature. Samples were then post-fixed by 1% osmium tetroxide for 2 h, dehydrated by graded ethanol and embedded in Epon 812 resin (Electron Microscopy Sciences, USA). Ultrathin sections were counterstained with uranyl acetate and lead citrate and visualized with JEM-1400FLASH Transmission Electron Microscope (JEOL, Japan).

2.9 | Animal model and AAV injection

AAV serotype 2/9 was used for the AP2S1 shRNA experiment. Murine shRNA sequences of AP2S1 were as follow: shAP2S1-1: GTTCAACTTCTACAAGGTTTA; shAP2S1-2: GATGCCAAGCACAC CAACTTT and shAP2S1-3: CACAACTTCGTAGAAGTGTTA. All three sequences were shown to reduce AP2S1 proteins (Figure S2) and shAP2S1-2 was selected for further animal testing. ShAP2S1-2 containing GFP-tagged AAV (pAAV-hSyn- EGFP-3XFLAG-shrna/AP2S1) was constructed by Obio (Shanghai, China) with particle concentration of 9.85 E + 12vg/ml. AAV without shRNA of AP2S1 was used as control. APPswe/PS1E9 (APP/PS1, C57BL/6; C3H) mice were obtained from the Jackson laboratory imported by Nanjing University (#004462). Wild-type (WT) littermates with the same background as APP/PS1 were verified and separated by genotyping. At 6 month of age, 40 male mice including 20 WT and 20 APP/PS1 were randomly assigned into the following four groups for AAV injection: WT for AAV control (WT-C) or shAP2S1 (WT-S), and APP/PS1 for AAV control (AD-C) or shAP2S1 (AD-S). AAV particles (0.5 μl at each site) were bilaterally injected into CA1 area of the hippocampus and the adjacent dentate gyrus as described previously.[25] Four weeks after the injection, mice were subjected to behavioral testing and then were sacrificed at

7.5 months after being anesthetized with inhalation of 5% isoflurane.[26] All animal procedures conformed to the Ethics Committee of the First Affiliated Hospital of Chongqing Medical University.

2.10 | Behavioral testing

Animal behavioral testing included Morris water maze (MWM) and open field tests (OFT). The MWM test was used to assess spatial memory.[19] Briefly, in 5 consecutive days, the mice underwent the platform trials and were allowed to find the hidden platform within 60 s. The time of each mouse to find the platform (escape latency) was recorded. On the sixth day, the hidden platform was removed, and the mice were given 60 s to find where the platform was originally placed. The frequency of passing the hidden platform (passing time) and the time stayed on the platform (staying time) were recorded. The open field test was performed as described previously.[27,28] In brief, mice were placed in an open field square apparatus, and were allowed to explore the surrounding for 5 min. Behavioral performance was recorded by image analyzing software (ANY-maze, Stoelting) and data were analyzed by two-way ANOVA with Tukey's post hoc test.

2.11 | Statistical analysis

All data were analyzed by GraphPad Prism 8.0 Software. Unless otherwise indicated, data were presented as mean ± standard error of mean (SEM) from at least three independent experiments. Statistical significance was determined by unpaired two-tailed Student's *t*-test, one-way or two-way ANOVA analysis. $p < 0.05$ was considered statistically significant.

3 | RESULTS

3.1 | AP2S1 knockdown or overexpression oppositely regulated APP protein level and amyloidogenesis

To explore whether AP2S1 might influence APP processing, we first assessed the protein levels of APP and the related proteolytic products sAPPβ and CTFs, in addition to those of BACE1 that is considered as rate-limiting enzyme in Aβ generation. As shown in Figure 1A, knockdown of AP2S1 (AP2S1 KD) significantly reduced the protein levels of APP, sAPPβ, BACE1 and CTFs in HEK293 cells that stably express human full-length APP695 (HEK-APP). Similarly, AP2S1 silencing also caused a significant reduction of APP and BACE1 protein levels in SH-SY5Y-APP cells that were derived from SH-SY5Y cells by stably expressing human full-length APP695 (Figure 1B). The reduced APP protein level by AP2S1 silencing was further found by immunofluorescence experiment in SH-SY5Y-APP cells (Figure 1C). It is reported that MOAB-2 monoclonal antibody specifically recognizes Aβ but not APP and CTFs.[29] Thus, we used this antibody for intracellular Aβ measurement. As shown in Figure 1D, the immunofluorescent intensity of MOAB-2 labeled Aβ was significantly reduced in SH-SY5Y-APP cells transiently transfected with AP2S1 siRNA. Further ELISA results also showed that both intracellular and extracellular Aβ42 levels were significantly decreased by AP2S1 KD in HEK-APP and SH-SY5Y-APP cells, whereas the corresponding Aβ40 levels were not markedly altered (Figure 1E,F).

To verify the effect of AP2S1 KD and to exclude the potential off-target effect of siRNA, we assessed APP and related protein levels in cells by overexpressing AP2S1. As shown in Figure 1G,H, overexpression of AP2S1 significantly increased the protein levels of APP, BACE1 and CTFs in HEK-APP or SH-SY5Y-APP cells. The enhanced protein level of APP was verified by immunofluorescent experiments (Figure 1I) and correspondingly, Aβ42 protein levels were significantly increased in SH-SY5Y-APP cells overexpressing AP2S1, whereas Aβ40 levels remained unchanged (Figure 1J). These results suggested that AP2S1 promoted Aβ generation by regulating APP protein level.

3.2 | AP2S1-mediated regulation involved lysosomal degradation

It is reported that Pitstop2 is an inhibitor of clathrin-dependent and -independent endocytosis,[30,31] whereas dynasore is an inhibitor of dynamin 1 that is reported to regulate APP endocytosis.[32] To determine whether AP2S1-mediated regulation of APP involves endocytosis, we assessed APP protein level in HEK-APP cells treated with Pitstop2 (15 μM for 15 min) or in SH-SY5Y-APP cells with dynasore (40 μM for 2 h). Both Pitstop2 and dynasore significantly inhibited the endocytosis of dextran (Figure S3). As shown in Figure 2A,B, the presence of Pitstop2 or dynasore did not significantly change the basal protein level of APP; and in cells treated with Pitstop2 or dynasore, the reduction of APP protein level by AP2S1 siRNA remained significant. EEA1 is a marker of early endosomes that receive endocytotic materials from cell surface.[33,34] We also found that the colocalization of APP with EEA1 was not altered by AP2S1 KD (Figure 2C), suggesting that endocytosis of APP was less likely involved in AP2S1-mediated regulation of APP protein. Because the protein level of APP could be influenced by the proteolytic processing of BACE1 and/or ADAM10, we also assessed the effect of AP2S1 KD on APP protein expression in HEK-APP cells treated with the BACE1 inhibitor LY2811376[35,36] in combination with the ADAM10 inhibitor GI254023X,[37] which are shown to alter the corresponding CTF levels.[20] As shown in Figure 2D, although LY2886721 and GI254023X together significantly increased the basal protein level of APP, they did not prevent the reduction of APP protein in HEK-APP cells transiently transfected with AP2S1 siRNA, indicating that AP2S1-mediated regulation of APP protein level was unrelated to the enzymatic activity of BACE1 and ADAM10. Moreover, the decreased levels of both the immature and mature forms of APP might be suggestive of an altered protein synthesis mechanism, we thus assessed the effect of AP2S1 in cells treated with protein synthesis inhibitor cycloheximide (CHX, 5 μM for 6 h).[38] As shown in Figure 2E, although CHX significantly reduced the basal protein level of APP, it did not prevent AP2S1 KD-induced reduction of APP.

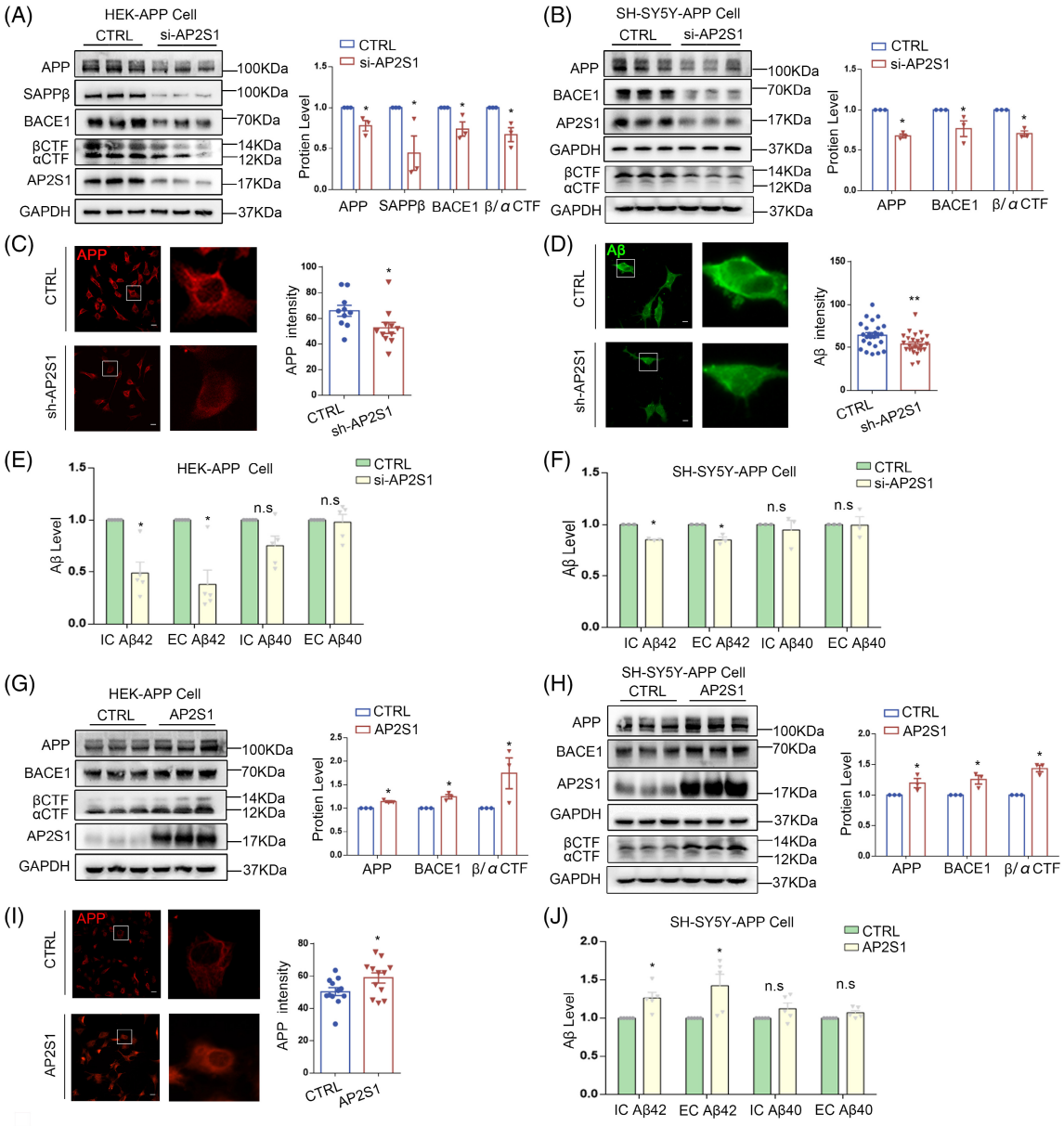

FIGURE 1 AP2S1 knockdown or overexpression oppositely regulates APP protein level and amyloidogenesis. A and B, Representative Western blots (left) and quantification (right) of APP, BACE1, CTFs and sAPPβ in HEK-APP (A) and SH-SY5Y-APP (B) cells transfected with control (CTRL) or AP2S1 siRNA for 48 h. For better detection of CTFs, cells were treated with the γ-secretase inhibitor DAPT (250 nM) for 24 h. (C and D) Representative immunofluorescent images show APP (C) and Aβ (D) protein intensity in SH-SY5Y-APP cells transfected with control or AP2S1 shRNA for 48 h ($n = 3$ biological replicates). Scale bar: 20 μm. (E and F) Aβ42 and Aβ40 levels were measured by ELISA in HEK-APP (E) and SH-SY5Y-APP (F) cells transfected with control or AP2S1 siRNA for 48 h. IC, intracellular; EC, extracellular. (G and H) Representative Western blots (left) and quantification (right) of APP, BACE1 and CTFs in HEK-APP (G) and SH-SY5Y-APP (H) cells transfected with control (CTRL) or AP2S1 plasmid for 48 h. (I) Representative immunofluorescent images show APP protein intensity in SH-SY5Y-APP cells transfected with control or AP2S1 plasmid for 48 h ($n = 3$ biological replicates). Scale bar: 20 μm. (J) Aβ42 and Aβ40 levels were measured by ELISA in SH-SY5Y-APP cells transfected with control or AP2S1 plasmid for 48 h. n.s., non-significant, $^*p < 0.05$, $^{**}p < 0.01$

Intracellular APP can be degraded by lysosome.[39] We next assessed whether AP2S1-mediated regulation of APP protein is associated with lysosomal degradation mechanism. As shown in Figure 2F,G, whereas bafilomycin A1 (BafA1, 100 nM for 5 h) or chloroquine (CQ, 100 μM for 6 h) alone significantly increased the basal protein level of APP, BafA1 but not CQ prevented the reduction of APP protein induced by AP2S1 siRNA. It is reported that mKeima is a coral-derived acid-stable fluorescent protein that emits the green and red signals at neutral and acidic pH, respectively.[23] Thus, we designed a plasmid construct in which APP was fused with mKeima. As shown in Figure 2H, mKeima reporter system was functional, as BafA1 significantly reduced the red (acidic) signals of APP. Compared with control, silencing of AP2S1 significantly increased the signal intensity of the acidic APP (Figure 2H). These results indicated that AP2S1-mediated regulation of APP was through lysosomal degradation.

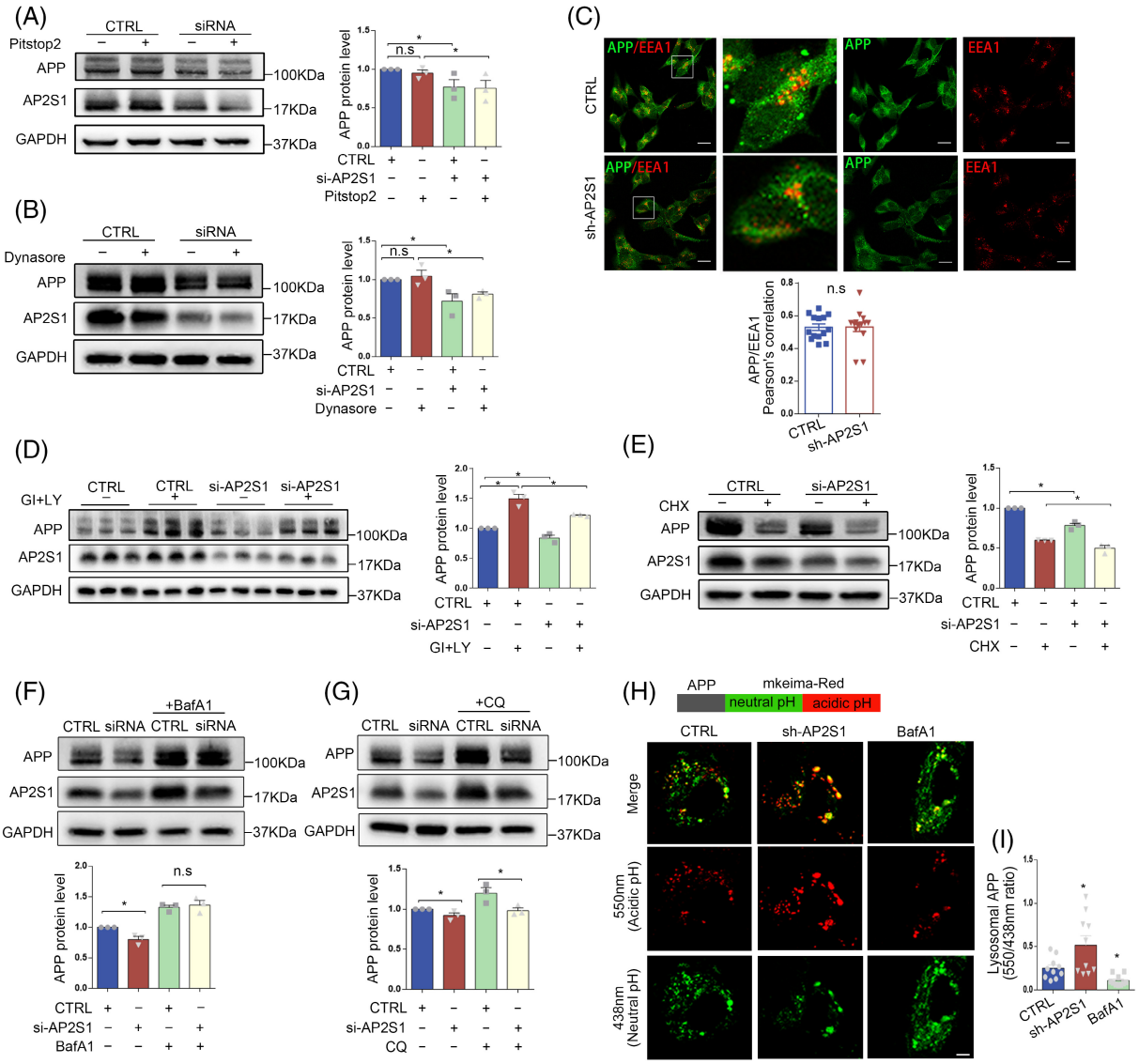

FIGURE 2 AP2S1-mediated regulation of APP involves lysosomal degradation. (A) Representative Western blots and quantification of APP proteins in HEK-APP cells transfected with control or AP2S1 siRNA for 48 h, in the absence or presence of clathrin-mediated endocytosis inhibitor Pitstop2 (15 μM for 15 min). (B) Representative Western blots and quantification of APP proteins in SH-SY5Y-APP cells transfected with control or AP2S1 siRNA for 48 h, in the absence or presence of dynamin 1 inhibitor dynasore (40 μM for 2 h). C, Representative fluorescent images show colocalization of APP with early endosomal marker EEA1 in SH-SY5Y-APP cells transfected with control or AP2S1 shRNA for 48 h, quantified by Pearson's co-localization coefficient ($n = 3$ biological replicates). Scale bar: 20 μm. (D) Representative Western blots and quantification of APP proteins in HEK-APP cells transfected with control or AP2S1 siRNA for 48 h, in the absence or presence of β-secretase inhibitor LY2811376 (LY, 50 μM) and α-secretase inhibitor GI254023X (GI, 10 μM). (E) Representative Western blots and quantification of APP protein levels in SH-SY5Y-APP cells transfected with control or AP2S1 siRNA for 48 h, in the absence or presence of protein synthesis inhibitor CHX (5 μM for 6 h). (F and G) Representative Western blots and quantification of APP proteins in HEK-APP cells transfected with control siRNA or AP2S1 siRNA for 48 h, in the absence or presence of lysosome inhibitor chloroquine (CQ, 100 μM for 6 h) or bafilomycin A1 (BafA1, 100 nM for 5 h), respectively. (H) Top, schematic illustration of APP-fused mKeima, a coral-derived acid-stable protein, emits green or red signaling at neutral or acidic pH, respectively. Bottom, representative fluorescent images of APP-mKeima signaling in SH-SY5Y cells transfected with control and AP2S1 shRNA for 48 h. Lysosomal inhibitor BafA1 (100 nM for 6 h) was used as positive control. (I) The 550 nm/438 nm signal intensity ratio of APP-mKeima represents lysosomal APP in live SH-SY5Y cells. (N = 3 biological replicates). Scale bar: 3 μm. n.s., non-significant, $^{*}p < 0.05$, $^{**}p < 0.01$

3.3 | AP2S1 silencing promoted the trans-localization of APP from late endosome to lysosome and LE-lyso fusion

The intracellular compartments of APP include early and late endosome, the Golgi complex and lysosome, where APP can be rapidly cleared.[40,41] We next assessed whether AP2S1-mediated degradation of APP is associated with the subcellular trafficking. The following markers for intracellular organelles were used: GM130 for *cis*-Golgi network (CGN),[42] RAB9 for late endosomes (LE),[39] and LAMP1 for lysosomes.[43] It seemed that AP2S1 did not affect the localization of APP with GM130 in SH-SY5Y-APP cells (Figure 3A). However, the

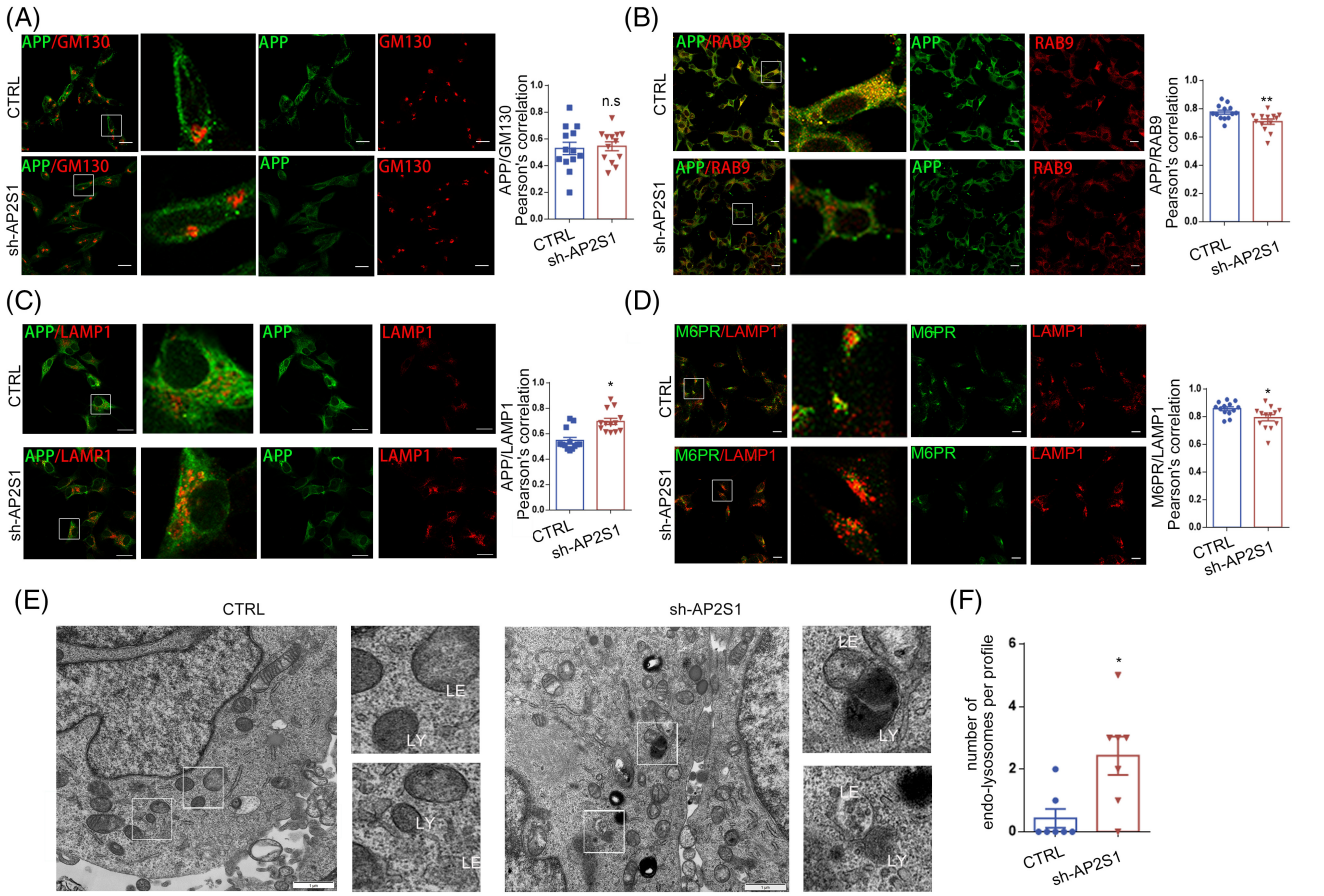

FIGURE 3 Silencing of AP2S1 promotes the trans-localization of APP from LE to lysosome and LE-lyso fusion. A to C, Representative fluorescent images show colocalization of APP with Golgi marker GM130 (A), late endosome marker RAB9 (B) and lysosome marker LAMP1 (C) in SH-SY5Y-APP cells transfected with control or AP2S1 shRNA for 48 h, quantified by Pearson's co-localization coefficient ($n = 3$ biological replicates). The right two columns show single-channel images of the protein labeling from the left (same as below). Scale bar: 20 μm. (D) Representative fluorescent images show the colocalization of LAMP1 and M6PR in SH-SY5Y-APP cells transfected with control or AP2S1 shRNA for 48 h, quantified by Pearson's co-localization coefficient ($n = 3$ biological replicates). Scale bar: 20 μm. (E) Representative transmission electron micrographs of SH-SY5Y-APP cells transfected with control or AP2S1 shRNA for 48 h. LE, late endosome; LY, lysosome; N, nucleus. Scale bar: 1 μm. (F) Quantification per cell profile shows an increase in average number of endo-lysosomes fusion in AP2S1 shRNA cells ($n = 3$ biological replicates). n.s., non-significant, $^*p < 0.05$, $^{**}p < 0.01$

reduced colocalization of APP with RAB9 was accompanied with the increased colocalization with LAMP1 (Figure 3B,C), indicating that AP2S1 KD promoted APP trafficking from LE to lysosomes. In contrast to AP2S1 KD, overexpression of AP2S1 resulted in a significant augmentation of RAB9-APP colocalization, whereas the colocalization of LAMP1 with APP was significantly reduced (Figure S4). It is reported that LAMP1-positive compartments could include endosomes in addition to lysosomes,[44,45] whereas mannose-6-phosphate receptor (M6PR) is found in endosome only but not lysosome.[46,47] To further distinguish the LAMP1-positive organelles between the endosome and lysosome, we assessed the colocalization of M6PR with LAMP1 in SH-SY5Y-APP cells transiently transfected with AP2S1 shRNA. As shown in Figure 3D, M6PR-positive LAMP1 labeling was significantly reduced by AP2S1 silencing, suggesting that a large fraction of the enhanced LAMP1-positive organelles were lysosomes.

The altered LE-lyso translocalization of APP by AP2S1 might reflect an altered LE-lyso fusion. As shown in Figure 3E,F, TEM images showed that more frequent LE-lyso fusion was observed in SH-SY5Y-APP cells transfected with AP2S1 shRNA relative to control. These results indicated that AP2S1 silencing promoted LE-lyso fusion.

3.4 | VPS41 was involved in APP degradation and trafficking regulated by AP2S1

The altered LE-lyso fusion prompted us to speculate that AP2S1-mediated regulation of APP trafficking might involve homotypic fusion and vacuole protein sorting (HOPS) complex, which play a key role in late endosome–lysosome fusion.[48] Thus, two HOPS proteins VPS41 and VPS16 that are known to regulate vacuolar morphology associated with neurological diseases were selected for further assessment[49,50] . As shown in Figure 4A,B, silencing of VPS41 indeed caused a significant increase of APP protein level at basal condition. Although AP2S1 KD reduced the basal protein level of APP, the

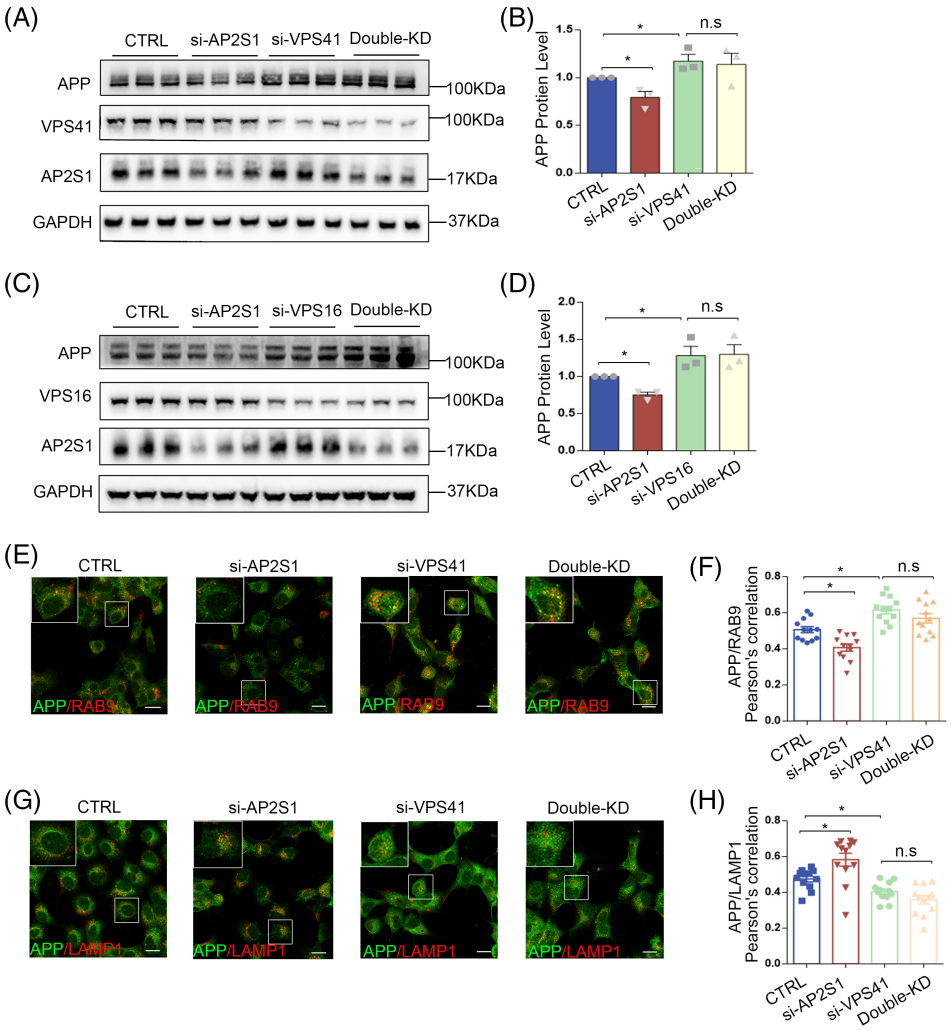

FIGURE 4 AP2S1-mediated APP trafficking involves tethering protein VPS41. (A and B) Representative Western blots (A) and quantification (B) of APP protein levels in HEK-APP cells transfected with control (CTRL) or AP2S1 siRNA, with or without the co-transfection of VPS41 siRNA ($n = 3$ biological replicates). (C and D) Representative Western blots (A) and quantification (B) of APP protein levels in HEK-APP cells transfected with control (CTRL) or AP2S1 siRNA, with or without the co-transfection of VPS16 siRNA ($n = 3$ biological replicates). (E and F) Representative fluorescent images show the colocalization of APP with RAB9 in HEK-APP cells transfected with siRNA of control, AP2S1 (si-AP2S1), VPS41 (si-VPS41) or AP2S1 + VPS41 (Double-KD) for 48 h, quantified by Pearson's co-localization coefficient ($n = 3$ biological replicates). Scale bar: 20 μm. (G and H) Representative fluorescent images show colocalization of APP with LAMP1 in HEK-APP cells transfected with siRNA of control, AP2S1 (si-AP2S1), VPS41 (si-VPS41) or AP2S1 + VPS41 (Double-KD) for 48 h, quantified by Pearson's co-localization coefficient ($n = 3$ biological replicates). Scale bar: 20 μm. n.s: non-significant, $^{*}p < 0.05$, $^{**}p < 0.01$

enhancement of APP level by VPS41 shRNA was not reversed by co-transfection of AP2S1 siRNA (Double KD), indicating that VPS41 prevented the effect of AP2S1 on APP degradation. Similarly, the effect of VPS41 was mimicked by VPS16, silencing of which caused an increased basal protein level of APP and prevented AP2S1-mediated regulation of APP (Figure 4C,D).

VPS41 was chosen to further determine whether HOPS complex is also involved in AP2S1-mediated translocalization of APP from LE to lysosome. As shown in Figure 4E,F, in HEK-APP cells, silencing of VPS41 alone increased the colocalization of RAB9 with APP, which was in line with previous report showing an accumulation of LE.[51] However, this increase was not significantly altered by additional co-transfection of AP2S1 siRNA (Double KD). Accordingly, as shown in Figure 4G,H, the colocalization of LAMP1 with APP was significantly reduced by VPS41 silencing alone, and this reduction was not reversed by AP2S1 siRNA (Double KD). These results indicated that AP2S1-mediated regulation of LE-lyso translocation of APP involved HOPS complex proteins VPS16 and VPS41, suggesting that AP2S1-mediated APP degradation was closely associated with LE-lyso fusion.

3.5 | LE-lyso fusion of APP by AP2S1 knockdown contributed to the improved cognition in APP/PS1 mice

To confirm the in vitro finding that LE-lyso fusion was involved in AP2S1-mediated regulation of APP, the AP2S1 shRNA sequence was

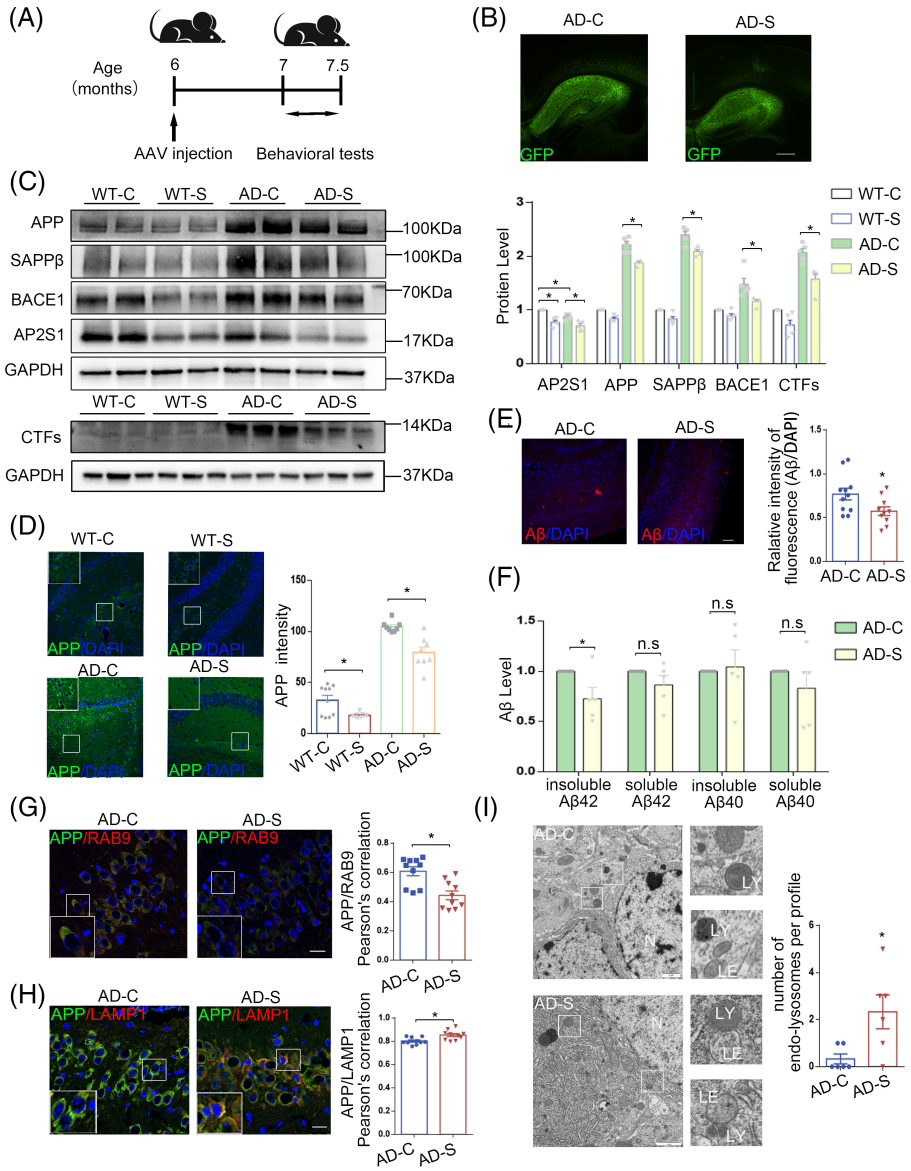

FIGURE 5 AP2S1 knockdown reduces APP protein and promotes LE-lyso fusion in APP/PS1 mice. (A) Schematic diagram shows the time course of animal manipulations. (B) Representative immunofluorescent images show GFP-tagged AAVs are successively delivered to the hippocampus. Scale bar: 100 μm. (C) Representative Western blots (top) and quantification (bottom) of APP, sAPPβ, BACE1, AP2S1 and CTFs protein levels in the hippocampus. WT-C/WT-S, wild-type mice injected with AAV control or AP2S1 shRNA; AD-C/AD-S, APP/PS1 mice injected with AAV control or AP2S1 shRNA ($n = 5$ for each group). (D) Representative immunofluorescent images show APP protein intensity in the hippocampus of WT-C, WT-S, AD-C and AD-S ($n = 4$ for each group). Green: APP; Blue: DAPI (nuclear marker). Scale bar: 75 μm. (E) Representative immunofluorescent image and quantification of Aβ intensity in AD-C and AD-S ($n = 3$ for each group). Red: Aβ; Blue: DAPI (nuclear marker). Scale bar: 75 μm. (F) The soluble and insoluble Aβ42 and Aβ40 levels in the hippocampus of AD-C and AD-S, respectively ($n = 5$ for each group). (G and H) Representative immunofluorescent images and quantification, which show the colocalization of APP with Rab9/Lamp1 in the hippocampus of AD-C and AD-S ($n = 4$ for each group). Scale bar: 20 μm. (I) Representative transmission electron micrographs of the hippocampus of AD-C and AD-S (left). Quantification per cell profile that exhibits an increase in average number of endo-lysosomes fusion in AD-S are shown on the right ($n = 3$ for each group). LE, late endosome; LY, lysosome; N, nucleus. Scale bar: 1 μm. n.s., non-significant, $^{*}p < 0.05$, $^{**}p < 0.01$

cloned into GFP-tagged AAV vector, which was injected bilaterally in the hippocampus of WT and AD mice at the age of 6 months (Figure 5A), respectively. The transfection efficiency was verified by GFP-positive signals shown in the hippocampus (Figure 5B). It is interesting to note that the basal AP2S1 protein levels were significantly decreased in AD-C relative to WT-C (Figure 5C). As expected, knockdown of AP2S1 significantly decreased the protein levels of APP, BACE1, sAPPβ and CTFs in WT-S relative to WT-C and in AD-S relative to AD-C, respectively (Figure 5C). In particular, the immunofluorescent intensity of APP was also significantly reduced in WT-S

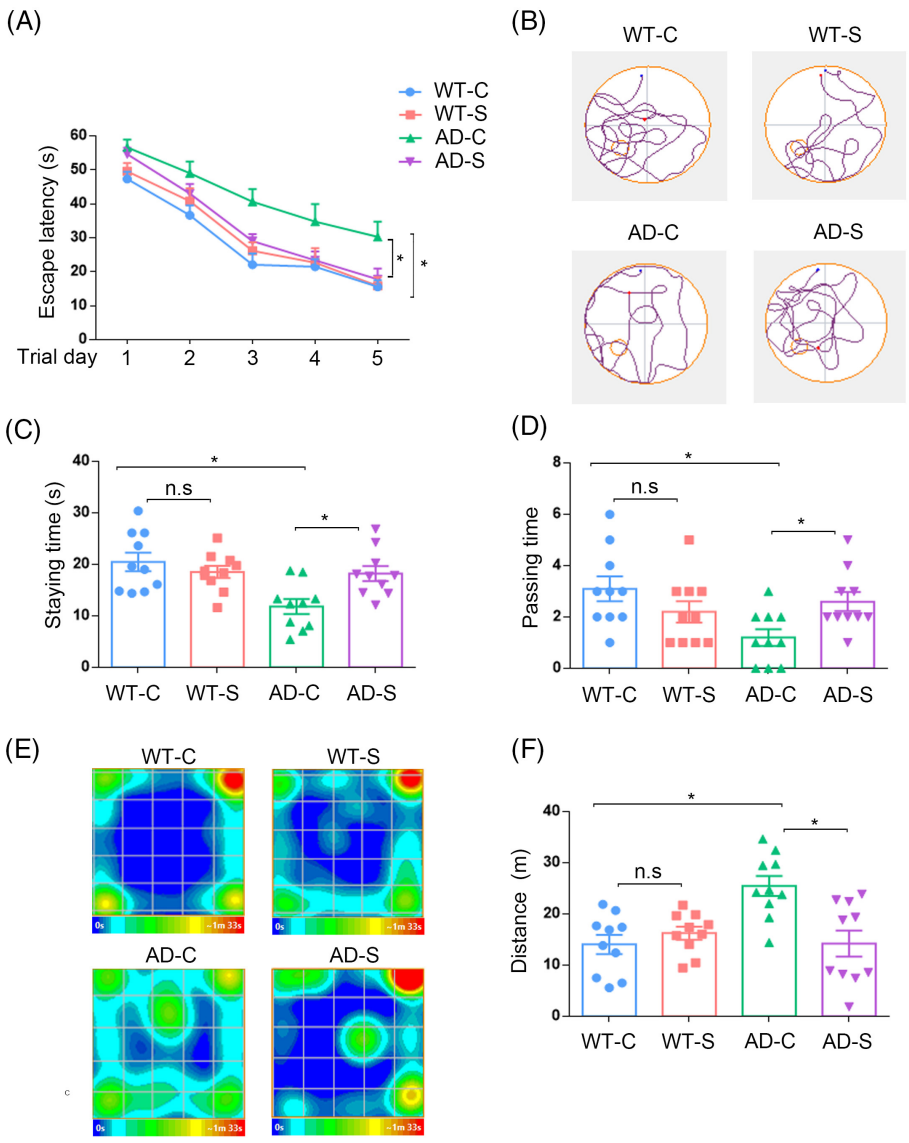

FIGURE 6 AAV-mediated AP2S1 knockdown improves learning and memory in APP/PS1 mice. (A) In the hidden platform tests, escape latency (the time spent on reaching the platform) relative to the training day was recorded by ANY-maze tracking Software ($n = 10$ mice). WT-C/WT-S: wild-type mice injected with AAV control or AP2S1 shRNA; AD-C/AD-S: APP/PS1 mice injected with AAV control or AP2S1 shRNA. (B) Representative road maps showing the movement trajectory of mice in the probe trial on the sixth day. (C and D) In the probe trial on the last day, the time period of staying (C, staying time) and the number of times crossed the site (D, passing times) were recorded by ANY-maze software ($n = 10$ mice). (E and F) In the open field tests, the representative heatmaps (E) and bar plot summary (F) show that AD-S mice exhibit significantly reduced hyperactivity relative to AD-C ($n = 10$ mice). n.s., non-significant, $^{*}p < 0.05$, $^{**}p < 0.01$

relative to WT-C and in AD-S relative to AD-C, respectively (Figure 5D); and the immunofluorescent intensity and size of the Aβ plaques were significantly reduced in AD-S mice compared with AD-C (Figure 5E, and Figure S5A). In line with the in vitro findings, the toxic insoluble Aβ42 levels were significantly decreased in AD-S compared with AD-C, whereas soluble Aβ42, soluble and insoluble Aβ40 levels were relatively unchanged (Figure 5F). Accordingly, astrocytic and microglial activation was significantly inhibited by AP2S1 KD, as the immunofluorescent intensities of glial fibrillary acidic protein (GFAP) and ionized calcium-binding adapter molecule 1 (Iba1) were significantly decreased in AD-S relative to AD-C (Figure S5B,C). The altered APP trafficking and LE-lyso fusion were further assessed by immunofluorescent and TEM experiments. As shown in Figure 5G,H, the colocalization of APP with RAB9 was significantly decreased, whereas that of APP with LAMP1 was significantly increased in the hippocampus of AD-S compared with AD-C. TEM images showed that the LE-lyso fusion events were more frequently seen in AD-S relative to AD-C (Figure 5I).

To determine whether knockdown of AP2S1 might alleviate cognitive decline in AD, we assessed cognitive function by using water maze and open field tests in WT and APP/PS1 mice. As shown in Figure 6A, the escape latency in the hidden platform test was significantly shorter in AD-S relative to AD-C. When the platform was removed during the probe trial, the staying time in the target quadrant and the passing time for crossing over the target site were significantly longer in AD-S than AD-C (Figure 6B–D). No significant differences were observed between WT-C and WT-S (Figure 6A–D). In the open field tests, AD-C mice were more active, which was in agreement with the hyperactivity of AD models,[28,52] and AD-S exhibited significantly reduced hyperactivity relative to AD-C (Figure 6E,F).

4 | DISCUSSION

AP2S1 is known to regulate endocytosis.[53] AP2S1 and AP2A1 (α-δ2) form a hemi-complex that binds to the dileucine-based sorting signals

and mediates protein internalization.[54] Structural analysis reveals that the hydrophobic pockets on AP2S1 are responsible for recognizing the dileucine motif.[55] However, evidences also show that AP2S1 has functions beyond endocytosis. For instance, AP2S1 mutants disrupt the polar transport of auxin (a plant hormone) in plant cells.[56] In drosophila, AP2S1 promotes synaptic vesicle recycling.[57] Mutations in AP2S1 impair its interaction with the α subunit and alter intracellular calcium signaling, which contributes to the phenotype of type 3 familial hypocalciuric hypercalcemia.[58,59] In line with these findings, inhibition of endocytosis by dynamin1 KD could increase surface APP but not total APP protein level.[60] In our study, the endocytosis inhibitor Pitstop2 or dynasore alone significantly inhibits the endocytosis of exogenously applied dextran (Figure S3), but neither of them alters the basal protein level of APP nor attenuates the effect of AP2S1 KD on APP (Figure 2A,B). Thus, our results support that AP2S1-mediated regulation of APP protein levels might be unrelated to endocytosis.

The current study reveals that the decreased APP by AP2S1 KD is closely associated with lysosomal function, which might be unrelated to either protein synthesis of APP or the enzymatic activity of BACE1/ADAM10, as the inhibitors of protein synthesis CHX and BACE1/ADAM10 fail to block this effect. The decreased protein level of APP is in agreement with the enhanced acidification of APP (Figure 2H), which is confirmed by that BafA1 prevents AP2S1-mediated degradation of APP (Figure 2F). Unexpectedly, although CQ is an autophagy inhibitor and increases the basal protein level of APP, it fails to attenuate the effect of AP2S1 on APP (Figure 2G). Whereas some studies reveal that CQ augments lysosomal pH,[61,62] others demonstrate that CQ does not alter lysosomal acidity,[63,64] which could be attributed to different cell types and drug concentrations and treating times. Nonetheless, as CQ inhibits autophagosome-lysosome fusion without altering endo-lysosomal trafficking of BSA,[64] and the majority of APP is degraded by endo-lyso rather than autophagic pathway,[65] the CQ results may not necessarily oppose the assumption that AP2S1 regulates the endo-lyso fusion.

The current study uses RAB9 for endosomal labeling, because the LE marker RAB7 also exists on lysosomes and autophagosome.[66,67] In comparison, RAB9 is mainly localized to EE, LE and TGN.[68,69] As the colocalization of APP with EEA1 (EE) and GM130 (Golgi network) was not affected by AP2S1 KD in our study, the reduced colocalization of RAB9 with APP suggests that APP localization in the pool of LE is reduced. This, together with the enhanced colocalization of APP-LAMP1, supports that APP is trafficked from LE to lysosome. Moreover, it is suggested that HOPS proteins including VPS16 and VPS41 form a link between endosome and lysosome.[48,70] Depletion of VPS16 leads to the impaired LE-lyso fusion[71,72]; and VPS41 knockdown hinders the delivery of endocytic cargo to lysosomes.[51] Interestingly, VPS41 protects cells from Aβ-induced toxicity in *Caenorhabditis elegans*, which involves lysosomal pathway[73]; and AP3, another AP complex, plays a role in VPS41-mediated lysosomal clearance of misfolded proteins and neuroprotection.[74,75] In our study, the LE-lyso fusion event is morphologically manifested by TEM, and functionally supported by that knockdown of VPS41 promotes APP accumulation in LE with the increased APP protein level under basal condition, and prevents AP2S1 KD-induced APP degradation and translocalization in vitro and in vivo. In addition, the reduced colocalization of M6PR with LAMP1 may also suggest that more LAMP1 is alternatively located in lysosome. Upon fusion with lysosome, M6PR is released from endosome,[76] whereas LAMP1 could remain attached at endo-lyso interface.

AP2S1 transcripts are significantly reduced rather than increased in the brain of AD patients (http://www.alzdata.org) and the hippocampus of the aged APP/PS1 mice.[77,78] In agreement, AP2S1 protein levels are significantly decreased in APP/PS1 mice relative to control (Figure 5C), suggesting that the downregulated expression of AP2S1 might play a compensative role. The in vivo experiments confirm the in vitro findings by that AAV-mediated delivery of AP2S1 shRNA significantly reduces the protein level of APP and amyloidogenesis, and increases the translocalization of APP with the enhanced LE-lyso fusion. Although accumulation of double-membrane autophagic vacuole is the prominent feature of AD,[79] the convergence of endosomal and authophagic pathway might be implicated in the processing of the pathologic CTFs.[12,80] It is suggested that endolysosomal trafficking and autophagy are mutually dependent in the pathophysiology of AD.[13,81]

Interestingly, the present study reveals that Aβ42 but not Aβ40 levels are selectively affected by AP2S1. The underlying mechanisms are currently unclear.[82] Early studies have demonstrated that intracellular compartmentation of APP, and the γ-secretase activity that acts on the distinct site of APP, contribute to the different levels of Aβ species.[83,84] Aβ42 could be localized to LE and lysosome of cultured cells[85] and is found in multivesicular bodies (MVB) in the brain of AD.[86,87] Importantly, lysosomal enzyme tripeptidyl peptidase 1 (TPP1) can directly proteolyze Aβ42 monomer.[88] Aβ42/Aβ40 ratio tends to increase with aging,[89,90] which is closely associated with lysosomal dysfunction.[91] Thus, it could be likely that the enhanced endo-lyso fusion favors the clearance of Aβ42.

The present study uncovers a different role of AP2S1 in APP processing relative to other subunits of AP2. The potential mechanisms are currently not well understood. One possibility is that AP2 subunits might function differently by forming hemi-complex. For instance, A1-S1 (α-δ2) and B1-M1 (β2-μ2) independently contribute to the endocytosis of synaptic vesicle.[92] α-δ2 shows strong binding to the dileucine-based motifs of several proteins, which bind weakly to β2-μ2.[54] However, AP2S1 may less likely cooperate with AP2A1 as a hemi-complex in APP processing, as AP2A1 silencing causes a significant increase rather than decrease of APP695 (neuronal type) level in H2 cells (human neuroglioma),[93] and CTF levels in N2a cells.[18] Although AP2A1 KO mice do not show significant alteration of APP protein, these mice exhibit an enhanced level of Aβ and CTFs.[16] Interestingly, the mRNA level of AP2S1 is not proportional to that of other AP2 subunits including AP2A1, with up to two-fold more transcripts of AP2S1 than AP2A1 in mice brain,[78,94,95] implying that AP2S1 might have functions beyond the 1:1 ratio of AP2S1/AP2A1 at protein level. Given that AP2S1 has functions beyond endocytosis (described above), it is tempting to speculate that the role of AP2S1 in regulating APP degradation might be independent of AP2A1.

A "kiss-and-run" model for endo-lyso fusion events has been proposed previously.[96,97] The mechanism of AP2 including AP2S1 in endocytosis involves membrane fission.[98] By analog, the existence of AP2S1 in endo-lyso organelles[18,99] might promote membrane dissociation (the "run" or fission process) between endosome and lysosome, whereas silencing of AP2S1 inhibits this process and favors the endo-lyso fusion (the "kiss" process), which might promote substance exchange and APP degradation in lysosome. Thus, the membrane fission controlled by AP2S1 might occur at not only cell surface but also endo-lyso interface. However, whether AP2S1 might work in concert with other AP2 subunits remains unclear, which requires further investigation.

In summary, the current study reveals that AP2S1 controls APP degradation through LE-lyso fusion mechanism. Inhibition of AP2S1 could promote the translocalization of APP from LE to lysosome, where the increased acidification might be responsible for the decreased protein level of APP and Aβ, contributing to the alleviation of cognitive decline in APP/PS1 mice. However, it is still too early to predict that the endo-lyso fusion mechanism involved in AP2S1 regulation has a therapeutic potential, when lysosomal acidification, in addition to other molecular alterations, becomes a major problem in the brain of AD.

AUTHOR CONTRIBUTIONS

Guo-Jun Chen and Xiao-Jiao Xiang designed the study. Qi-Xin Wen performed the experiments and analyzed the data. Biao-Luo, Xiao-Yong Xie, Gui-Feng Zhou, Jian Chen, Li Song, Yue Liu, Shi-Qi Xie, Long Chen and Kun-Yi Li provided assistance with the research. Guo-Jun Chen and Qi-Xin Wen wrote the manuscript.

ACKNOWLEDGMENTS

This work was supported by the National Nature Science Foundation of China (81971030) and Chongqing Education commission (KJZD-K201900404) to Guo-Jun Chen, by National Nature Science Foundation of China (82201578) to Xiao-Jiao Xiang, and by T Postgraduate Research and Innovation Project of Chongqing (CYB19146) to Li Song. All experiments were conducted in compliance with the ARRIVE Guidelines.

CONFLICT OF INTEREST

The authors declare no conflict of interest.

PEER REVIEW

The peer review history for this article is available at https://publons.com/publon/10.1111/tra.12874.

DATA AVAILABILITY STATEMENT

All data in this study will be made available upon reasonable request and approval by Guo-Jun Chen and Qi-Xin Wen. Requests can be made by email to the corresponding author.

ORCID

Qi-Xin Wen https://orcid.org/0000-0003-1864-9978

REFERENCES

1. Long J, Holtzman D. Alzheimer disease: an update on pathobiology and treatment strategies. *Cell*. 2019;179(2):312-339.
2. Sun X, Bromley-Brits K, Song W. Regulation of beta-site APP-cleaving enzyme 1 gene expression and its role in Alzheimer's disease. *J Neurochem*. 2012;120(suppl 1):62-70.
3. Cacace R, Sleegers K, Van Broeckhoven C. Molecular genetics of early-onset Alzheimer's disease revisited. *Alzheimers Dement*. 2016;12(6):733-748.
4. Bignante E, Heredia F, Morfini G, Lorenzo A. Amyloid β precursor protein as a molecular target for amyloid β-induced neuronal degeneration in Alzheimer's disease. *Neurobiol Aging*. 2013;34(11):2525-2537.
5. Zhang X, Song W. The role of APP and BACE1 trafficking in APP processing and amyloid-β generation. *Alzheimers Res Ther*. 2013;5(5):46.
6. Toh W, Gleeson P. Dysregulation of intracellular trafficking and endosomal sorting in Alzheimer's disease: controversies and unanswered questions. *Biochem J*. 2016;473(14):1977-1993.
7. Guimas Almeida C, Sadat Mirfakhar F, Perdigão C, Burrinha T. Impact of late-onset Alzheimer's genetic risk factors on beta-amyloid endocytic production. *Cell Mol Life Sci*. 2018;75(14):2577-2589.
8. Van Acker ZP, Bretou M, Annaert W. Endo-lysosomal dysregulations and late-onset Alzheimer's disease: impact of genetic risk factors. *Mol Neurodegener*. 2019;14(1):20.
9. Ubelmann F, Burrinha T, Salavessa L, et al. Bin1 and CD2AP polarise the endocytic generation of beta-amyloid. *EMBO Rep*. 2017;18(1):102-122.
10. Fjorback AW, Seaman M, Gustafsen C, et al. Retromer binds the FANSHY sorting motif in SorLA to regulate amyloid precursor protein sorting and processing. *J Neurosci*. 2012;32(4):1467-1480.
11. Klinger SC, Højland A, Jain S, et al. Polarized trafficking of the sorting receptor SorLA in neurons and MDCK cells. *FEBS J*. 2016;283(13):2476-2493.
12. Nixon RA. Amyloid precursor protein and endosomal-lysosomal dysfunction in Alzheimer's disease: inseparable partners in a multifactorial disease. *FASEB J*. 2017;31(7):2729-2743.
13. Peric A, Annaert W. Early etiology of Alzheimer's disease: tipping the balance toward autophagy or endosomal dysfunction? *Acta Neuropathol*. 2015;129(3):363-381.
14. Canagarajah BJ, Ren X, Bonifacino JS, Hurley JH. The clathrin adaptor complexes as a paradigm for membrane-associated allostery. *Protein Sci*. 2013;22(5):517-529.
15. Mettlen M, Chen P, Srinivasan S, Danuser G, Schmid S. Regulation of clathrin-mediated endocytosis. *Annu Rev Biochem*. 2018;87:871-896.
16. Bera S, Camblor-Perujo S, Calleja Barca E, et al. AP-2 reduces amyloidogenesis by promoting BACE1 trafficking and degradation in neurons. *EMBO Rep*. 2020;21(6):e47954.
17. Schneider A, Rajendran L, Honsho M, et al. Flotillin-dependent clustering of the amyloid precursor protein regulates its endocytosis and amyloidogenic processing in neurons. *J Neurosci*. 2008;28(11):2874-2882.
18. Tian Y, Chang JC, Fan EY, Flajolet M, Greengard P. Adaptor complex AP2/PICALM, through interaction with LC3, targets Alzheimer's APP-CTF for terminal degradation via autophagy. *Proc Natl Acad Sci U S A*. 2013;110(42):17071-17076.
19. Zhu BL, Long Y, Luo W, et al. MMP13 inhibition rescues cognitive decline in Alzheimer transgenic mice via BACE1 regulation. *Brain*. 2019;142(1):176-192.
20. Chen J, Luo B, Zhong BR, et al. Sulfuretin exerts diversified functions in the processing of amyloid precursor protein. *Genes Dis*. 2021;8(6):867-881.
21. Hicks DA, Makova NZ, Gough M, Parkin ET, Nalivaeva NN, Turner AJ. The amyloid precursor protein represses expression of acetylcholinesterase in neuronal cell lines. *J Biol Chem*. 2013;288(36):26039-26051.

22. Aung KT, Yoshioka K, Aki S, Ishimaru K, Takuwa N, Takuwa Y. The class II phosphoinositide 3-kinases PI3K-C2α and PI3K-C2β differentially regulate clathrin-dependent pinocytosis in human vascular endothelial cells. *J Physiol Sci*. 2019;69(2):263-280.
23. Katayama H, Kogure T, Mizushima N, Yoshimori T, Miyawaki AJC. A sensitive and quantitative technique for detecting autophagic events based on lysosomal delivery. *Chem Biol*. 2011;18(8):1042-1052.
24. Lojk J, Bregar VB, Rajh M, et al. Cell type-specific response to high intracellular loading of polyacrylic acid-coated magnetic nanoparticles. *Int J Nanomedicine*. 2015;10:1449-1462.
25. Kiyota T, Yamamoto M, Schroder B, et al. AAV1/2-mediated CNS gene delivery of dominant-negative CCL2 mutant suppresses gliosis, beta-amyloidosis, and learning impairment of APP/PS1 mice. *Mol Ther*. 2009;17(5):803-809.
26. Liu X, Zhang W, Alkayed NJ, et al. Lack of sex-linked differences in cerebral edema and aquaporin-4 expression after experimental stroke. *J Cereb Blood Flow Metab*. 2008;28(12):1898-1906.
27. Tsuda MC, Ogawa S. Long-lasting consequences of neonatal maternal separation on social behaviors in ovariectomized female mice. *PLoS One*. 2012;7(3):e33028.
28. Sanchez PE, Zhu L, Verret L, et al. Levetiracetam suppresses neuronal network dysfunction and reverses synaptic and cognitive deficits in an Alzheimer's disease model. *Proc Natl Acad Sci U S A*. 2012;109(42):E2895-E2903.
29. Youmans KL, Tai LM, Kanekiyo T, et al. Intraneuronal Abeta detection in 5xFAD mice by a new Abeta-specific antibody. *Mol Neurodegener*. 2012;7:8.
30. Dutta D, Williamson C, Cole N, Donaldson J. Pitstop 2 is a potent inhibitor of clathrin-independent endocytosis. *PLoS One*. 2012;7(9):e45799.
31. Rosenbaek L, Kortenoeven M, Aroankins T, Fenton R. Phosphorylation decreases ubiquitylation of the thiazide-sensitive cotransporter NCC and subsequent clathrin-mediated endocytosis. *J Biol Chem*. 2014;289(19):13347-13361.
32. Carey RM, Balcz BA, Lopez-Coviella I, Slack BE. Inhibition of dynamin-dependent endocytosis increases shedding of the amyloid precursor protein ectodomain and reduces generation of amyloid beta protein. *BMC Cell Biol*. 2005;6:30.
33. Scott C, Vacca F, Gruenberg J. Endosome maturation, transport and functions. *Semin Cell Dev Biol*. 2014;31:2-10.
34. Dilsizoglu Senol A, Tagliafierro L, Gorisse-Hussonnois L, et al. Protein interacting with amyloid precursor protein tail-1 (PAT1) is involved in early endocytosis. *Cell Mol Life Sci*. 2019;76(24):4995-5009.
35. Willem M, Tahirovic S, Busche MA, et al. eta-Secretase processing of APP inhibits neuronal activity in the hippocampus. *Nature*. 2015;526(7573):443-447.
36. Guo Y, Huang F, Sun W, et al. Unprecedented polycyclic polyprenylated acylphloroglucinols with anti-Alzheimer's activity from St. John's wort. *Chem Sci*. 2021;12(34):11438-11446.
37. Kuang X, Zhou HJ, Thorne AH, Chen XN, Li LJ, Du JR. Neuroprotective effect of ligustilide through induction of alpha-secretase processing of both APP and klotho in a mouse model of Alzheimer's disease. *Front Aging Neurosci*. 2017;9:353.
38. Zhong BR, Zhou GF, Song L, et al. TUFM is involved in Alzheimer's disease-like pathologies that are associated with ROS. *FASEB J*. 2021;35(5):e21445.
39. Tam J, Pasternak S. Imaging the intracellular trafficking of APP with photoactivatable GFP. *J Vis Exp*. 2015;105:e53153.
40. Tam J, Seah C, Pasternak SJM. The amyloid precursor protein is rapidly transported from the Golgi apparatus to the lysosome and where it is processed into beta-amyloid. *Mol Brain*. 2014;7:54.
41. Yamazaki T, Koo E, Selkoe DJ. Trafficking of cell-surface amyloid beta-protein precursor. II. Endocytosis, recycling and lysosomal targeting detected by immunolocalization. *J Cell Sci*. 1996;109(pt 5):999-1008.
42. Nozawa N, Daikoku T, Koshizuka T, Yamauchi Y, Yoshikawa T, Nishiyama Y. Subcellular localization of herpes simplex virus type 1 UL51 protein and role of palmitoylation in Golgi apparatus targeting. *J Virol*. 2003;77(5):3204-3216.
43. Cabana VC, Bouchard AY, Senecal AM, et al. RNF13 dileucine motif variants L311S and L312P interfere with endosomal localization and AP-3 complex association. *Cell*. 2021;10(11).
44. Cheng X, Xie Y, Zhou B, Huang N, Farfel-Becker T, Sheng Z. Characterization of LAMP1-labeled nondegradative lysosomal and endocytic compartments in neurons. *J Cell Biol*. 2018;217(9):3127-3139.
45. Falcón-Pérez JM, Nazarian R, Sabatti C, Dell'Angelica EC. Distribution and dynamics of Lamp1-containing endocytic organelles in fibroblasts deficient in BLOC-3. *J Cell Sci*. 2005;118(pt 22):5243-5255.
46. Ghosh P, Dahms NM, Kornfeld S. Mannose 6-phosphate receptors: new twists in the tale. *Nat Rev Mol Cell Biol*. 2003;4(3):202-212.
47. Díaz E, Pfeffer SJC. TIP47: a cargo selection device for mannose 6-phosphate receptor trafficking. *Cell*. 1998;93(3):433-443.
48. van der Beek J, Jonker C, van der Welle R, Liv N, Klumperman J. CORVET, CHEVI and HOPS – multisubunit tethers of the endo-lysosomal system in health and disease. *J Cell Sci*. 2019;132(10).
49. Steel D, Zech M, Zhao C, et al. Loss-of-function variants in HOPS complex genes VPS16 and VPS41 cause early onset dystonia associated with lysosomal abnormalities. *Ann Neurol*. 2020;88(5):867-877.
50. Monfrini E, Zech M, Steel D, Kurian MA, Winkelmann J, Di Fonzo A. HOPS-associated neurological disorders (HOPSANDs): linking endo-lysosomal dysfunction to the pathogenesis of dystonia. *Brain*. 2021;144(9):2610-2615.
51. Pols MS, ten Brink C, Gosavi P, Oorschot V, Klumperman J. The HOPS proteins hVps41 and hVps39 are required for homotypic and heterotypic late endosome fusion. *Traffic*. 2013;14(2):219-232.
52. Lerdkrai C, Asavapanumas N, Brawek B, et al. Intracellular Ca stores control in vivo neuronal hyperactivity in a mouse model of Alzheimer's disease. *Proc Natl Acad Sci U S A*. 2018;115(6):E1279-E1288.
53. Gulbranson DR, Crisman L, Lee M, et al. AAGAB controls AP2 adaptor assembly in clathrin-mediated endocytosis. *Dev Cell*. 2019;50(4):436-446.e435.
54. Doray B, Lee I, Knisely J, Bu G, Kornfeld S. The gamma/sigma1 and alpha/sigma2 hemicomplexes of clathrin adaptors AP-1 and AP-2 harbor the dileucine recognition site. *Mol Biol Cell*. 2007;18(5):1887-1896.
55. Kelly BT, McCoy AJ, Späte K, et al. A structural explanation for the binding of endocytic dileucine motifs by the AP2 complex. *Nature*. 2008;456(7224):976-979.
56. Fan L, Hao H, Xue Y, et al. Dynamic analysis of Arabidopsis AP2 σ subunit reveals a key role in clathrin-mediated endocytosis and plant development. *Development*. 2013;140(18):3826-3837.
57. Choudhury SD, Mushtaq Z, Reddy-Alla S, et al. sigma2-Adaptin facilitates basal synaptic transmission and is required for regenerating endo-exo cycling pool under high-frequency nerve stimulation in Drosophila. *Genetics*. 2016;203(1):369-385.
58. Nesbit MA, Hannan FM, Howles SA, et al. Mutations in AP2S1 cause familial hypocalciuric hypercalcemia type 3. *Nat Genet*. 2013;45(1):93-97.
59. Gorvin CM, Metpally R, Stokes VJ, et al. Large-scale exome datasets reveal a new class of adaptor-related protein complex 2 sigma subunit (AP2σ) mutations, located at the interface with the AP2 alpha subunit, that impair calcium-sensing receptor signalling. *Hum Mol Genet*. 2018;27(5):901-911.
60. Zhu L, Su M, Lucast L, et al. Dynamin 1 regulates amyloid generation through modulation of BACE-1. *PLoS One*. 2012;7(9):e45033.
61. Fedele AO, Proud CG. Chloroquine and bafilomycin A mimic lysosomal storage disorders and impair mTORC1 signalling. *Biosci Rep*. 2020;40(4).
62. Jacquin E, Leclerc-Mercier S, Judon C, Blanchard E, Fraitag S, Florey O. Pharmacological modulators of autophagy activate a parallel

noncanonical pathway driving unconventional LC3 lipidation. *Autophagy*. 2017;13(5):854-867.
63. Lu S, Sung T, Lin N, Abraham RT, Jessen BA. Lysosomal adaptation: how cells respond to lysosomotropic compounds. *PLoS One*. 2017; 12(3):e0173771.
64. Mauthe M, Orhon I, Rocchi C, et al. Chloroquine inhibits autophagic flux by decreasing autophagosome-lysosome fusion. *Autophagy*. 2018;14(8):1435-1455.
65. Swaminathan G, Zhu W, Plowey ED. BECN1/Beclin 1 sorts cell-surface APP/amyloid β precursor protein for lysosomal degradation. *Autophagy*. 2016;12(12):2404-2419.
66. Wandinger-Ness A, Zerial M. Rab proteins and the compartmentalization of the endosomal system. *Cold Spring Harb Perspect Biol*. 2014; 6(11):a022616.
67. Jimenez-Orgaz A, Kvainickas A, Nägele H, et al. Control of RAB7 activity and localization through the retromer-TBC1D5 complex enables RAB7-dependent mitophagy. *EMBO J*. 2018;37(2):235-254.
68. Kucera A, Borg Distefano M, Berg-Larsen A, et al. Spatiotemporal resolution of Rab9 and CI-MPR dynamics in the endocytic pathway. *Traffic*. 2016;17(3):211-229.
69. Hutagalung AH, Novick PJ. Role of Rab GTPases in membrane traffic and cell physiology. *Physiol Rev*. 2011;91(1):119-149.
70. Brocker C, Kuhlee A, Gatsogiannis C, et al. Molecular architecture of the multisubunit homotypic fusion and vacuole protein sorting (HOPS) tethering complex. *Proc Natl Acad Sci U S A*. 2012;109(6): 1991-1996.
71. Galmes R, ten Brink C, Oorschot V, et al. Vps33B is required for delivery of endocytosed cargo to lysosomes. *Traffic*. 2015;16(12):1288-1305.
72. Wartosch L, Gunesdogan U, Graham SC, Luzio JP. Recruitment of VPS33A to HOPS by VPS16 is required for lysosome fusion with endosomes and autophagosomes. *Traffic*. 2015;16(7):727-742.
73. Griffin EF, Yan X, Caldwell KA, Caldwell GA. Distinct functional roles of Vps41-mediated neuroprotection in Alzheimer's and Parkinson's disease models of neurodegeneration. *Hum Mol Genet*. 2018;27(24): 4176-4193.
74. Harrington AJ, Yacoubian TA, Slone SR, Caldwell KA, Caldwell GA. Functional analysis of VPS41-mediated neuroprotection in *Caenorhabditis elegans* and mammalian models of Parkinson's disease. *J Neurosci*. 2012;32(6):2142-2153.
75. Rehling P, Darsow T, Katzmann D, Emr SD. Formation of AP-3 transport intermediates requires Vps41 function. *Nat Cell Biol*. 1999;1(6): 346-353.
76. Griffiths G, Hoflack B, Simons K, Mellman I, Kornfeld S. The mannose 6-phosphate receptor and the biogenesis of lysosomes. *Cell*. 1988; 52(3):329-341.
77. Xu M, Zhang DF, Luo R, et al. A systematic integrated analysis of brain expression profiles reveals YAP1 and other prioritized hub genes as important upstream regulators in Alzheimer's disease. *Alzheimers Dement*. 2018;14(2):215-229.
78. Yang J, Long Y, Xu D, et al. Age- and nicotine-associated gene expression changes in the hippocampus of APP/PS1 mice. *J Mol Neurosci*. 2019;69(4):608-622.
79. Yu WH, Cuervo AM, Kumar A, et al. Macroautophagy—a novel β-amyloid peptide-generating pathway activated in Alzheimer's disease. *J Cell Biol*. 2005;171(1):87-98.
80. Tian Y, Chang JC, Greengard P, Flajolet M. The convergence of endosomal and autophagosomal pathways: implications for APP-CTF degradation. *Autophagy*. 2014;10(4):694-696.
81. Funk KE, Mrak RE, Kuret J. Granulovacuolar degeneration (GVD) bodies of Alzheimer's disease (AD) resemble late-stage autophagic organelles. *Neuropathol Appl Neurobiol*. 2011;37(3):295-306.
82. Qiu T, Liu Q, Chen YX, Zhao YF, Li YM. Aβ42 and Aβ40: similarities and differences. *J Pept Sci*. 2015;21(7):522-529.
83. Hartmann T, Bieger SC, Brühl B, et al. Distinct sites of intracellular production for Alzheimer's disease A beta40/42 amyloid peptides. *Nat Med*. 1997;3(9):1016-1020.
84. Greenfield JP, Tsai J, Gouras GK, et al. Endoplasmic reticulum and trans-Golgi network generate distinct populations of Alzheimer beta-amyloid peptides. *Proc Natl Acad Sci U S A*. 1999;96(2):742-747.
85. Omtri RS, Davidson MW, Arumugam B, Poduslo JF, Kandimalla KK. Differences in the cellular uptake and intracellular itineraries of amyloid beta proteins 40 and 42: ramifications for the Alzheimer's drug discovery. *Mol Pharm*. 2012;9(7):1887-1897.
86. Takahashi RH, Milner TA, Li F, et al. Intraneuronal Alzheimer abeta42 accumulates in multivesicular bodies and is associated with synaptic pathology. *Am J Pathol*. 2002;161(5):1869-1879.
87. Takahashi RH, Nagao T, Gouras GK. Plaque formation and the intraneuronal accumulation of β-amyloid in Alzheimer's disease. *Pathol Int*. 2017;67(4):185-193.
88. Solé-Domènech S, Rojas AV, Maisuradze GG, Scheraga HA, Lobel P, Maxfield FR. Lysosomal enzyme tripeptidyl peptidase 1 destabilizes fibrillar Aβ by multiple endoproteolytic cleavages within the β-sheet domain. *Proc Natl Acad Sci U S A*. 2018;115(7):1493-1498.
89. Miners JS, Jones R, Love S. Differential changes in Aβ42 and Aβ40 with age. *J Alzheimers Dis*. 2014;40(3):727-735.
90. Zhao Q, Lu J, Yao Z, et al. Upregulation of Aβ42 in the brain and bodily fluids of rhesus monkeys with aging. *J Mol Neurosci*. 2017; 61(1):79-87.
91. Wong SQ, Kumar AV, Mills J, Lapierre LR. Autophagy in aging and longevity. *Hum Genet*. 2020;139(3):277-290.
92. Gu M, Liu Q, Watanabe S, et al. AP2 hemicomplexes contribute independently to synaptic vesicle endocytosis. *Elife*. 2013;2:e00190.
93. Prabhu Y, Burgos PV, Schindler C, Farías GG, Magadán JG, Bonifacino JS. Adaptor protein 2-mediated endocytosis of the β-secretase BACE1 is dispensable for amyloid precursor protein processing. *Mol Biol Cell*. 2012;23(12):2339-2351.
94. Yang J, Liu AY, Tang B, et al. Chronic nicotine differentially affects murine transcriptome profiling in isolated cortical interneurons and pyramidal neurons. *BMC Genomics*. 2017;18(1):194.
95. Simpson JE, Ince PG, Shaw PJ, et al. Microarray analysis of the astrocyte transcriptome in the aging brain: relationship to Alzheimer's pathology and APOE genotype. *Neurobiol Aging*. 2011;32(10):1795-1807.
96. Bright NA, Gratian MJ, Luzio JP. Endocytic delivery to lysosomes mediated by concurrent fusion and kissing events in living cells. *Curr Biol*. 2005;15(4):360-365.
97. Trivedi PC, Bartlett JJ, Pulinilkunnil T. Lysosomal biology and function: modern view of cellular debris bin. *Cell*. 2020;9(5).
98. Renard HF, Johannes L, Morsomme P. Increasing diversity of biological membrane fission mechanisms. *Trends Cell Biol*. 2018;28(4): 274-286.
99. Rong Y, Liu M, Ma L, et al. Clathrin and phosphatidylinositol-4,-5-bisphosphate regulate autophagic lysosome reformation. *Nat Cell Biol*. 2012;14(9):924-934.

SUPPORTING INFORMATION

Additional supporting information can be found online in the Supporting Information section at the end of this article.

How to cite this article: Wen Q-X, Luo B, Xie X-Y, et al. AP2S1 regulates APP degradation through late endosome–lysosome fusion in cells and APP/PS1 mice. *Traffic*. 2023; 24(1):20-33. doi:10.1111/tra.12874